JURNAL UPI

Indonesian Journal of Science & Technology

Journal homepage: http://ejournal.upi.edu/index.php/ijost/

IJoST Indonesian Journal of Science & Technology

Active Disturbance Rejection Control of Wearable Lower-Limb System Based on Reduced ESO

Nasir Ahmed Alawad[1], *Amjad J. Humaidi*[2], *Abdulkareem Sh. Mahdi Al-Obaidi*[3*], *Ahmed Sabah Alaraji*[4]

[1]Department of Computer Engineering, Faculty of Engineering, Mustansiriyah University, Baghdad, Iraq
[2]Department of Control and System Engineering, University of Technology, Baghdad, Iraq
[3]School of Engineering, Faculty of Innovation and Technology, Taylor's University, Taylor's Lakeside Campus, Subang Jaya, Selangor DE, Malaysia
[4]Department of Computer Engineering, University of Technology, Baghdad, Iraq
Correspondence: E-mail: abdulkareem.mahdi@taylors.edu.my

A B S T R A C T

Wearable robots are commonly used for rehabilitation and they are made to fit the human body to assist persons who are unable to help themselves. The design of controllers became necessary to enhance the dynamic motion of these exoskeleton systems when worn by patients. In this study, active disturbance rejection control (ADRC) with reduced-order extended state observer (RESO) has been proposed for motion control of exoskeleton knee-assisting device to eliminate the phase lag induced by full-order extended state observer (FESO). The design analysis of RESO-based ADRC has been presented and a computer simulation has been conducted to verify the effectiveness of the proposed controller. A comparison study has been made between ADRC based on RESO and that based on FESO in terms of transient and robustness characteristics. The simulated results showed that the RESO-based ADRC gives better transient and load rejection capabilities compared to the controller with FESO.

A R T I C L E I N F O

Article History:
Submitted/Received 11 Feb 2022
First revised 07 Mar 2022
Accepted 28 May 2022
First available online 30 May 2022
Publication date 01 Sep 2022

Keyword:
ADRC control,
Exoskeleton system,
Reduced-order extended state observer,
Robustness,
Tracking control.

1. INTRODUCTION

Active disturbance rejection control (ADRC) is a modern control technology that is based on a standard PID control theory (Han, 1988; Humaidi & Badr, 2018a; Al-Obaidi, 2021a; Babalola & Omolafe, 2022a; Babalola & Omolafe, 2022b; Castiblanco *et al*., 2021; Khairudin *et al*., 2020). The extended state observer (ESO) is a type of observer that is commonly employed in ADRC. It can be used to estimate generalized disturbances, including lumped unknown dynamics and uncertain disturbances, and then the generalization perturbations are immediately compensated by a state feedback controller (Caifen & Wen 2021). ESOs have been widely employed in many sophisticated uncertain systems, such as spacecraft structure systems (Yang *et al*., 2014), permanent magnet synchronous motor (PMSM) servo systems (Liu & Li, 2012), hypersonic vehicles, and multi-agent systems (Yang *et al*., 2015). Because of their good estimating properties and capacity to adjust, other structures of observers exist in addition to ESOs, such as the unknown input observer (UIO), disturbance observer (DOB), and perturbation observer (POB), adaptive observer, and sliding mode observer (Hameed *et al*., 2019, Hassan *et al*., 2020, Falah *et al*., 2020, Djamel & Mefoud, 2019).

The ESO in ADRC decreases the amount of noise in the feedback loop, but it also introduces phases lag like a low-pass filter. The phases lag is increased as the order of the systems is increased. In previous study, the disturbance and unmolded dynamics associated with induction motors are considered as an extra state variable and the reduced-order ADRC (RADRC) approach is advised to further reduce the phase lag induced by ESO. For multivariable chemical process systems, the (RESO) is designed to replace the full order ESO in ADRC and reduce phase lag while maintaining excellent performance with robustness and adaptability to disturbances. In previous works (Nowak *et al*., 2018; Huang & Xue, 2014), the robust tuning rules have been presented for RADRC with first plus dead time processes. The RESO in RADRC does not appear at the plant output, but only its derivatives and the generalized disturbance. Because the measured variables are also tracked in full-order ESO, their order is lower than the usual ADRC method with a full-order ESO. Due to the limited availability of literature on RADRC tuning, (Caifen & Wen 2021) developed a novel parameter tuning method based on the original ARDC. The RESO is applied to improve the performance of motion control of the exoskeleton system for knee joint rehabilitation controlled by ADRC by eliminating the phase lag.

Other techniques and methodologies can be pursued to extend this study for future work (Yung *et al*., 2016; Eftekhari & Al-Obaidi, 2019; Eftekhari *et al*., 2020; Kulshreshtha & Al-Obaidi, 2020; Al-Obaidi, 2021; Ali *et al*., 2020; Al-Obaidi, A. S. M. *et al*., 2021b; Eftekhari *et al*., 2023).

This article is organized in the following. The dynamics of the exoskeleton are described in Section 3. The main concept of the RADRC is presented in Section 4. The proposed ADRC based on RESO is discussed in Section 5. The numerical results and discussion of the exoskeleton system based on RESO-based ADRC are shown in Section 6. Finally, concluding remarks based on simulated results are highlighted in Section 7.

2. MODELLING OF EXOSKELETON SYSTEM FOR LOWER-LIMB

The Exoskeleton Knee system is a wearable robotic device that is used to restore or enhance the function of the lower limb (Shawgi *et al*., 2022; Alawad *et al*., 2022). **Figure 1** depicts the geometric representation of leg motion at the knee joint (Aljuboury *et al*., 2022).

DOI: https://doi.org/10.17509/ijost.v7i2
p- ISSN 2528-1410 e- ISSN 2527-8045

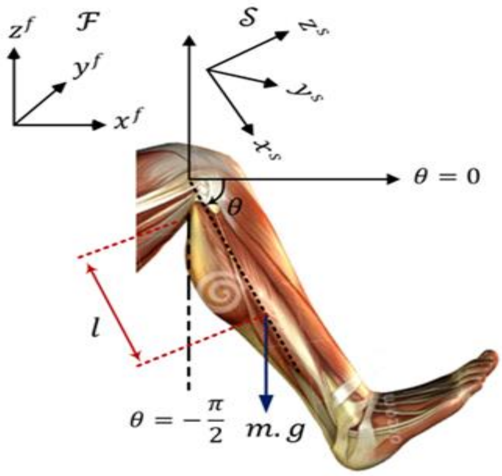

Figure 1. The geometric representation of leg orientation at the knee joint (AljubourY *et al.*, 2022).

According to **Figure 1**., the parameters m and l are the mass and length of the shank, respectively, while g is the gravitational acceleration. The exoskeleton and human model were modelled as a system of rigid bodies with one degree of freedom for the knee part. The nonlinear dynamic for the exoskeleton and human model with one joint, at the knee, is determined through the use of the Euler–Lagrange method. The dynamic modelling of the system can be expressed as follows (Aljubory *et al.*, 2022; Bkekri *et al.*, 2019; Mefoued,2015) (see Equation (1)):

$$J\ddot{\theta} = -\tau_g cos\theta - A\ sgn\dot{\theta} - B\dot{\theta} + \tau_h + \tau \quad (1)$$

where, θ is the knee joint angle between the actual position of the shank and the full extension position, $\dot{\theta}$ and $\ddot{\theta}$ are, respectively, the knee joint angular velocity and acceleration. J, A, B, τ_g, τ and $\tau_h$are the leg inertia, solid friction coefficient, viscous friction coefficient, gravity torque, actuating torque, and human torque which are applied to the Knee-Exoskeleton system at the knee level, respectively.

Letting x_1 and $x_2$represent the variables θ and $\dot{\theta}$, the above equation can be written in state variable (see Equation (2)):

$$\dot{x}_1 = x_2 \quad (2)$$
$$\dot{x}_2 = f + b_o\,\tau$$

where $b_o = 1/J$ and f represents the lumped term of uncertainties and nonlinearities, which is given by Equation (3):

$$f = \frac{1}{J}\left[-\tau_g cosx_1 - A\ sgnx_2 - B\ x_2 + \tau_h\right] \quad (3)$$

3. METHODOLOGY

In order to decrease the effect of phase–lag on the stability of controlled system based on ADRC and to reduce the sensitivity of observer against noise, two observer approaches have been proposed for Exoskeleton-knee system. The first approach utilizes full Extended State Observer, while the other uses Reduced Extended State Observer.

4. ADRC WITH FULL-ORDER ESO

The PD-based ADRC is a mixture of a tracking differentiator, an extended State Observer (ESO), and a proportional-Derivative controller (Han, 1995). In this study, linear ADRC has been adopted. In this version of ADRC, linear functions are used, and hence the linear gains, rather than nonlinear gains, have to be determined according to the bandwidth concept (Caifen & Wen 2021). The general block diagram of ADRC based on the PD controller is shown in **Figure 2**.

DOI: https://doi.org/10.17509/ijost.v7i2
p- ISSN 2528-1410 e- ISSN 2527-8045

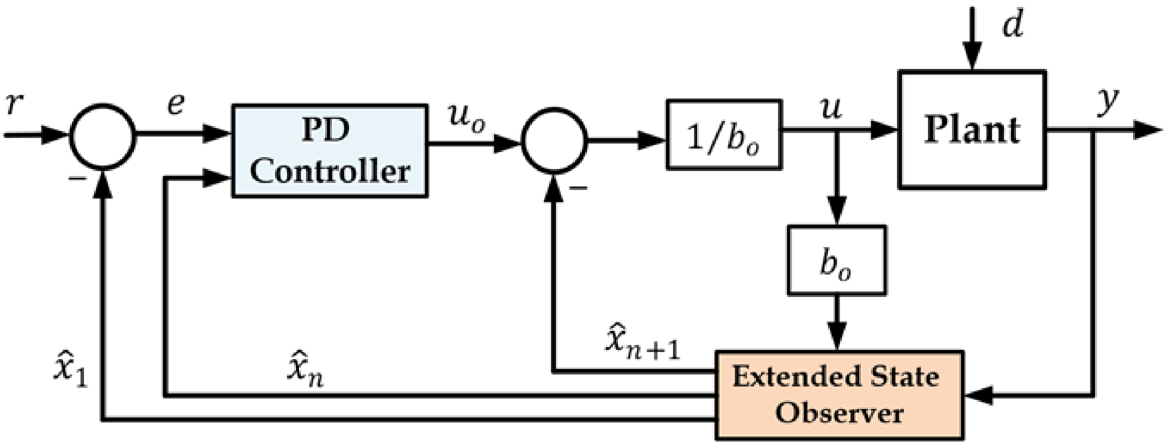

Figure 2. Block-diagram of general ADRC.

Consider the n-th full order system described by (see Equation (4)):

$$y^{(n)} = f\left(y^{(n-1)}, y^{(n-2)}, \dots, y, d, t\right) + b_o u \tag{4}$$

where y, u, b_o, and f represent the system output, the control law, the nominal input matrix, and the term that stands the lumping uncertainties and nonlinearities, respectively. The basic operation of ADRC is based on predicting the unknown generalized disturbance f. This task is attributed to the ESO observer. This core part of the control structure permits an approximate estimate of total disturbance.

Therefore, the full order ESO (FESO) is used to estimate f and all states of the system, $(x_1, x_2, \dots, x_n, x_{n+1})$, and hence it will estimate the variables $(y, \dot{y}, \dots., y^{n-1}, f)$. Then, according to (Caifen & Wen 2021), the augmented state-space model of Equation (4) can be represented as (see Equation (5)):

$$\dot{x} = Ax + B\,u + E\,\dot{f} \tag{5}$$

$$y = C\,x$$

where,

$$A = \begin{bmatrix} 0 & 1 \cdots & 0 \\ \vdots & \ddots & \vdots \\ 0 & \cdots & 0 \end{bmatrix}, B = \begin{bmatrix} 0 \\ \vdots \\ b_o \\ 0 \end{bmatrix}, E = \begin{bmatrix} 0 \\ \vdots \\ 1 \end{bmatrix},$$

$$C = [1\ 0 \cdots 0]$$

The extended state observer has synthesized based on a previous work (Humaidi & Badr, 2018a) (see Equation (6))

$$\dot{\hat{x}} = A\,\hat{x} + B\,u + L\,(y - \hat{y}) \tag{6}$$

Here, $\hat{x}$ is the estimated state vector of x, $\hat{y}$ is the estimated output of the system y, L is the observer gains vector, which is given by $L = [L_1\ L_2 \cdots\ L_{n+1}]^T$. The elements of the observer gain matrix can be expressed in terms of observer bandwidth (ω_o). The well-tuned outputs of ESO $\hat{x}_i$ are close to x_i, then we get Equation (7)

$$\hat{x}_{n+1} \approx x_{n+1} \approx f \tag{7}$$

From Equation (7), the generalized perturbation can be compensated using the following the control law:

$$u = \frac{u_o - \hat{x}_{n+1}}{b_o} \tag{8}$$

where, u_o is part of control signal u as indicated in **Figure 2.** Then, substituting Equation (8) into Equation (4) to deduce Equation (9):

$$y^{(n)} = f - \hat{x}_{n+1} + u_o \tag{9}$$

According to Equation (8), the control signal u_o can be expressed in terms of elements of the PD controller (see Equation (10))

$$u_o = K_p(r - \hat{x}_1) - K_{d1}\,\hat{x}_2 + \cdots + K_{dn}\,\hat{x}_n \tag{10}$$

where, K_p and K_{di} $(i = 1, \cdots, n)$ are the proportional and derivative gains, respectively. It has been shown the terms of PD controller are related to the bandwidth of the controlled system ω_c. A large value of ω_c leads to increased speed of dynamic. However, higher bandwidth might cause the

DOI: https://doi.org/10.17509/ijost.v7i2
p- ISSN 2528-1410 e- ISSN 2527-8045

controlled system to oscillate or possibly become unstable. Therefore, ω_c has a direct impact on performance, robustness, and noise sensitivity requirements (Amjad *et al*., 2018a; Han, 1998).

However, other recent and efficient optimization techniques can be used to tune the gains of PD controllers like Particle Swarm Optimization (PSO), Ant Colony Optimization, Whale Optimization Algorithm (WOA), Social Spider Optimization (SSO), Grey-Wolf optimization (GWO) (Hassan & Rashad, 2011; Al-Qassar *et al*., 2021a; Al-Qassar *et al*., 2021b; Humaidi *et al*., 2020; Humaidi *et al*., 2021; Luay, 2020; Mustafa *et al*., 2021; Humaidi *et al*., 2022). These optimization techniques are characterized by finding optimal values of gains in terms of minimizing the tracking errors.

5. ADRC BASED ON REDUCED ESO

Observers act as a low pass filter in the feedback loop, reducing external noise. However, this noise rejection property has an adverse effect on the closed-loop system by adding a phase lag. When the system order increases, the observer gains (L) expand as well, providing more phases lag at the same time. Due to the loss of loop stability, phase lag is not a useful result of compensation. Therefore, the problem of increased phase lag due to using full-order ESO can be solved by using a reduced-order ESO.

This leads to reduced ADRC (RADRC), which can be illustrated clearly in **Figure 3.** Therefore, compared to ADRC, the RADRC will reduce the effect of the observer's phase lag on the controlled system. The implementation of RESO is an ADRC framework is simple, as long as the system output (y) is provided and measured. It is not necessary to use all estimates produced by ESO, but only use the estimated state $\hat{x}_{n+1}$ that represents the lumped uncertainties. Therefore, for the nth-order system and if the measurements $(y, \dot{y}, \ldots., y^{n-1})$ are available, Equation (10) can be written as Equation (11):

$$u_o = K_p(r-y) - K_{d1}\dot{y} + \cdots + K_{dn}y^{(n-1)} \quad (11)$$

In the case of the exoskeleton system (second-order), Equation (11) can be expressed as (see Equation (12))

$$u_o = K_p(r-y) - K_{d1}\dot{y} \quad (12)$$

The ESO works to feedback only the $\hat{x}_3$. This proposed structure is demonstrated in **Figure 3.**

In the sense of adopting this proposed ESO, the observer of ADRC is reduced to one degree and the observer gain is defined by $(L_3 = \omega_o^3)$, while in the case of FESO, where there are two estimate states $(x_{1,}x_2)$, it requires two gains to be determined $(L_1 = 2\omega_0, L_2 = \omega_o^2)$.

Pursuing the analysis of literature (Han, 1998), the bandwidth ω_c is related to settling time t_s of the closed-loop system according to the following Equation (13):

$$\omega_c = 10/t_s \quad (13)$$

In this application, the specification of settling time of controlled system application is chosen to be $t_s = 0.408$ s. As such, the bandwidth ω_c can be determined according to the above equation to have a value of $\omega_c = 24.5$rad/s. If one chooses the observer bandwidth to be equal $\omega_o = 4\,\omega_c$, then it easy to calculate the elements of observer matrix gains $(L_1,\ L_2,\ L_3)$ and the values of controller gains using the expressions $k_p = \omega_c^2$, and $k_d = 2\,\omega_c$.

DOI: https://doi.org/10.17509/ijost.v7i2
p- ISSN 2528-1410 e- ISSN 2527-8045

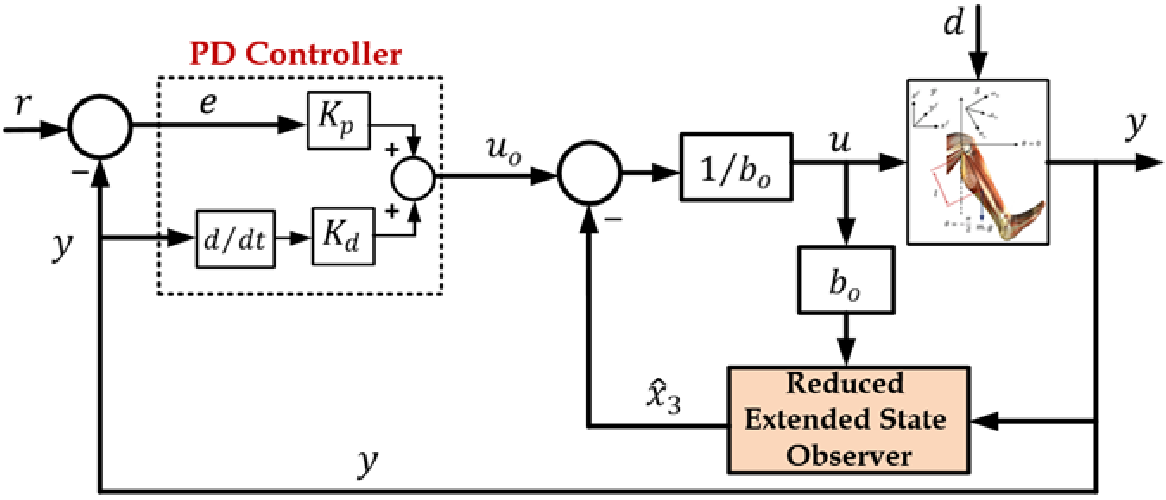

Figure 3. Block diagram of ADRC based on Reduced ESO for Knee-rehabilitation device.

6. COMPUTER SIMULATION

The numerical simulation has been conducted to verify the effectiveness of the proposed controller. Indeed, it is good for taking into account that the exoskeleton device is worn by a healthy person, who is 27 years old, weighing 90 Kg and measuring 1.87 m.

According to this real case study, the parameters exoskeleton system has been listed in **Table 1** (Mefoued *et al.*, 2015; Djamel & Mefoud, 2019).

6.1. Case I: Step Input

In this part, the effectiveness of the ADRC controller has been investigated with two types of ESO: Reduced ESO (RESO) and Full ESO (FESO). The controlled exoskeleton system has been subjected to step input.

Figure 4 shows responses of joint angular positions due to both structures of controllers. It is evident that, with the same bandwidth of observers, both controllers give good tracking performance. However, the ADRC based on RESO has a faster transient with a settling time of 0.25 s, as compared to the controller with FESO, which results in 1.2 s. settling time.

Furthermore, the figure clearly shows that there is a reduction in phase lag due to applying RESO for ADRC compared to that based on FESO. This leads to improved estimating capability of RESO-based ADRC.

The next scenario investigates the impact of load exertion on the transient characteristics of joint behavior based on ADRC with two schemes of ESO. **Figure 5** shows the change in responses due to step-load application of (10 N.m) at time 2 s.

Table 1. The parameters of the exoskeleton system for knee rehabilitation.

Parameter	Value
Inertia (J)	0.348 kg.m^2
Viscous Friction Coefficient (B)	0.872 N.m.s/rad
Solid Friction Coefficient (A)	0.998 N.m
Gravity Torque (τ_g)	3.445 N.m

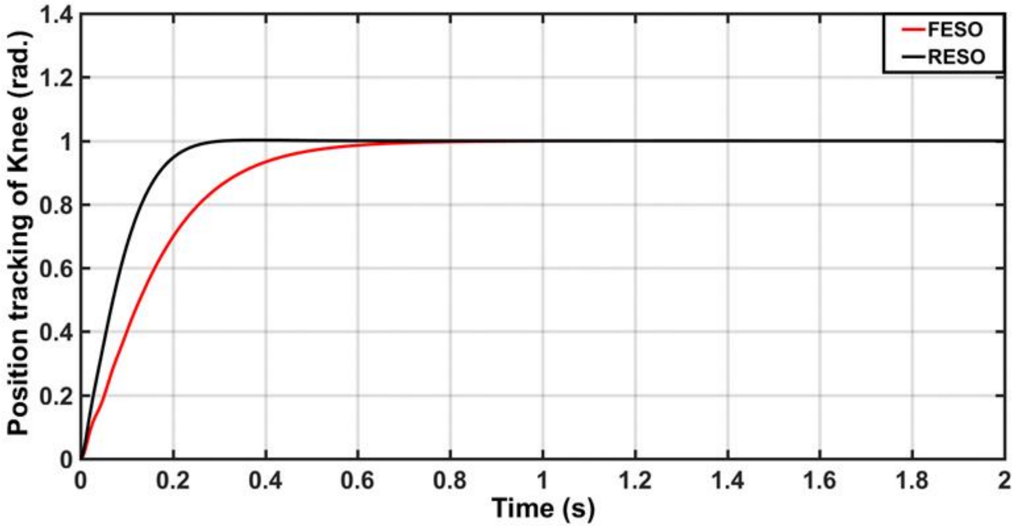

Figure 4. Transient responses of joint angles based on ADRC with RESO and FESO (without disturbance).

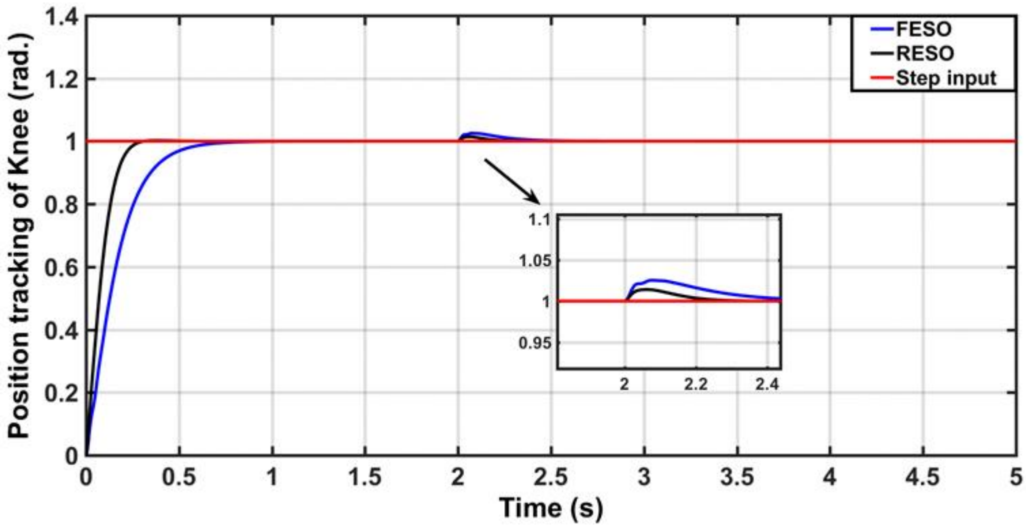

Figure 5. Transient responses of joint angular position with ADRC based on RESO and FESO under load change.

The ADRC based on RESO shows better robustness characteristics than that based on FESO. The response based on RESO returns quicker and has less peak than that based on FESO upon load change. Therefore, one can conclude that the RESO-based ADRC has better load rejection capability than its opponent.

The above argument and conclusion are clarified based on the dynamics of tracking errors due to ADRC with RESO and FESO as shown in **Figure 6** The figure indicates how RESO could improve the tracking error and robustness characteristics as compared to FESO.

Figure 7 shows the control signals (torque) applied to the exoskeleton system resulting from both schemes of observer-based controllers. It is evident from the figure that less control effort with less chattering can be obtained with ADRC based on RESO over that based on FESO. One can conclude that better control effort can be obtained by RESO compared to FESO.

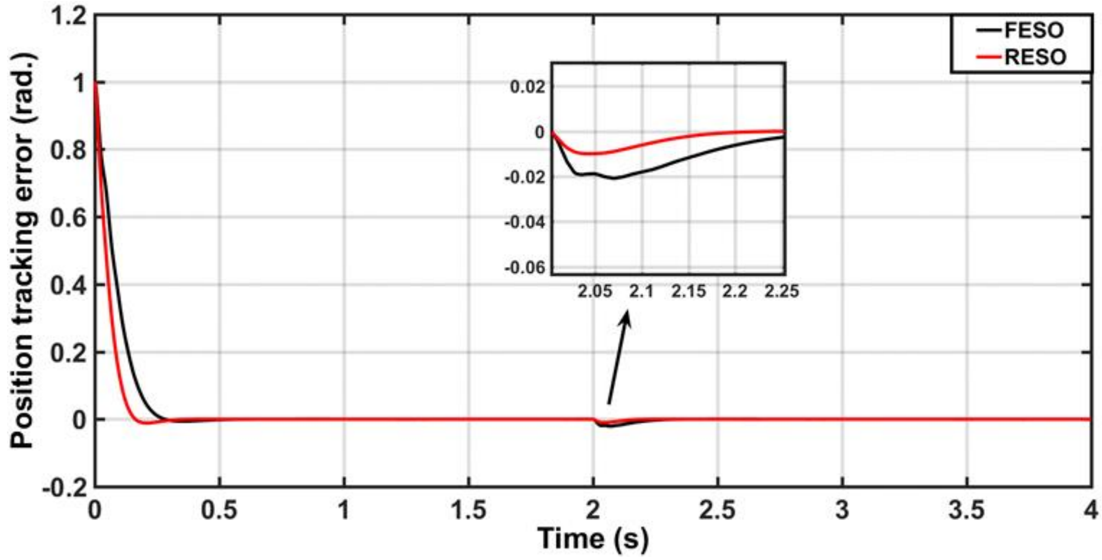

Figure 6. Dynamics of tracking errors due to ADRC based on RESO and FESO under load exertion.

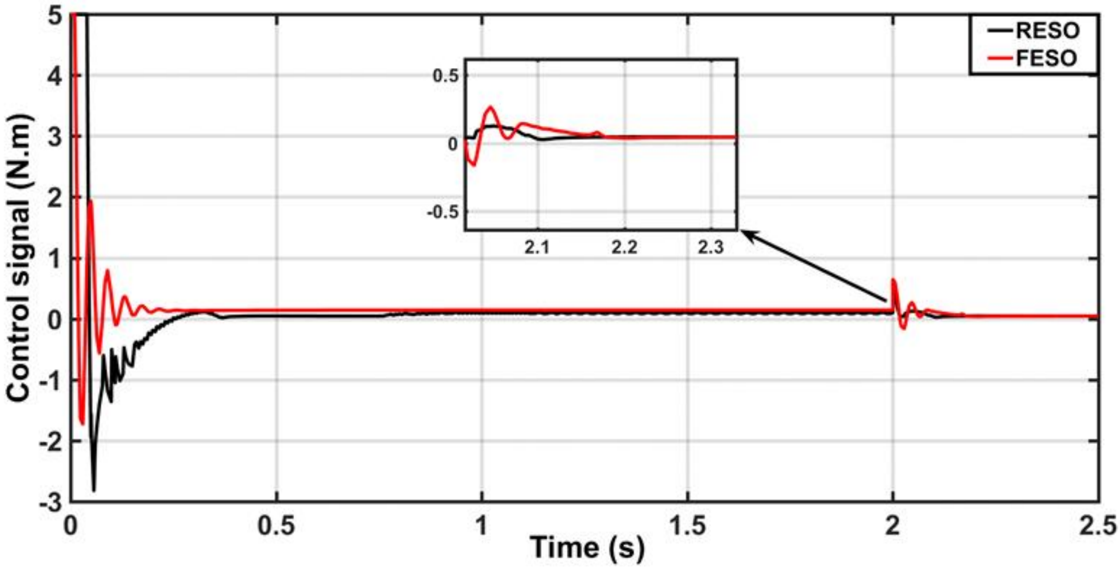

Figure 7. Behaviors of control signals resulting from ADRC based on both RESO and FESO in the presence of external uncertainty (disturbance).

6.2. Case II: Real Clinical Reference Input

In rehabilitation exercises of exoskeleton systems of knee joint motion, there are different reference trajectories are applied to a controlled system like sin and cosine functions. In this test, a real (clinical) reference trajectory has been chosen (Zhou *et al.*, 2013; Sumit *et al.*, 2020; Long *et al.*, 2017):

$$r(t) = 0.766\cos\ (0.\pi\ t) - 0.099\cos(\pi t) - 0.342\sin\ (\pi t) - 0.219\cos(2\pi t) + 0.168\sin(2\pi t) + 0.008\cos(3\pi t) + 0.084\sin(3\pi t) - 26.127$$

Using this real-like reference input, the previous analysis can be conducted for controlled systems based on two structures of observers. **Figure 8** shows the transient behaviors of joint angles due to ADRCs based

DOI: https://doi.org/10.17509/ijost.v7i2
p- ISSN 2528-1410 e- ISSN 2527-8045

on RESO and FESO with a disturbance-free system.

Figure 9 gives the corresponding error dynamics according to **Figure 8** To evaluate the performance, the Root Mean Square of Error (RMSE) is used as the measuring index. Based on simple calculations, it has been shown that the ADRC with RESO gives less value of RMSE (0.5495) compared to that based on FESO (1.9318).

The behaviors of actuating signals (torques) for exoskeleton devices, due to the schemes of observer-based ADRC, are shown in **Figure 10.** The actuating signal based on FESO shows a higher peak, at the startup of transient response, as compared to RESO. However, in this scenario, the requirements of control efforts are higher than that based on the step reference trajectory for both controllers. In the next computer simulation, the performances of both observer-based controllers are assessed when the system is subjected to a random load of Gaussian distribution (mean=0, variance =1).

Figure 11 and **Figure 12** show the tracking responses of joint angles and their corresponding errors, respectively, for the knee rehabilitation system in the presence of load disturbance. According to the calculation of RMSE, it has been shown that the RESO-based ADRC gives better tracking accuracy than ADRC based on FESO, where the first controller records (RMSE = 0.5514), while the latter one records (RMSE = 1.915).

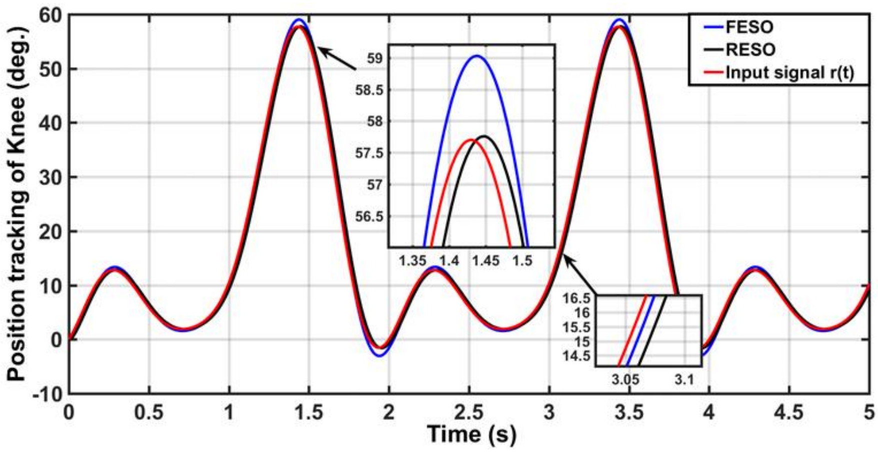

Figure 8. Transient responses of joint angular position with ADRC based on RESO and FESO (without disturbance).

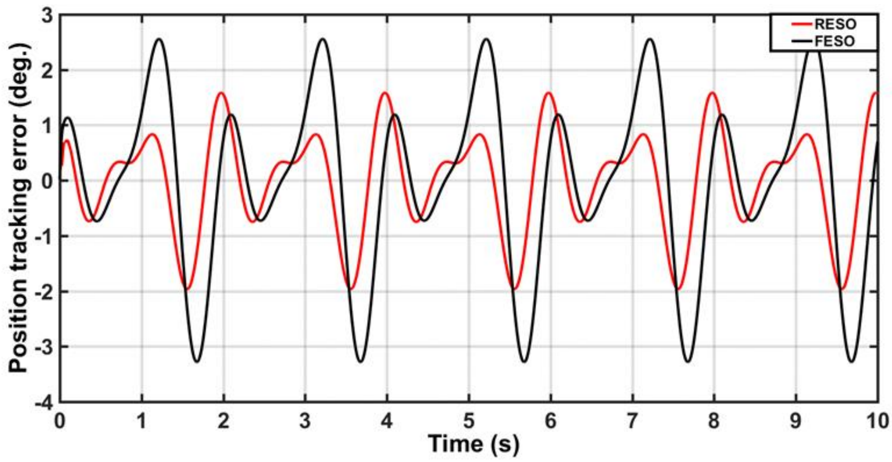

Figure 9. Dynamics of tracking errors due to ADRC based on RESO and FESO (without disturbance).

DOI: https://doi.org/10.17509/ijost.v7i2
p- ISSN 2528-1410 e- ISSN 2527-8045

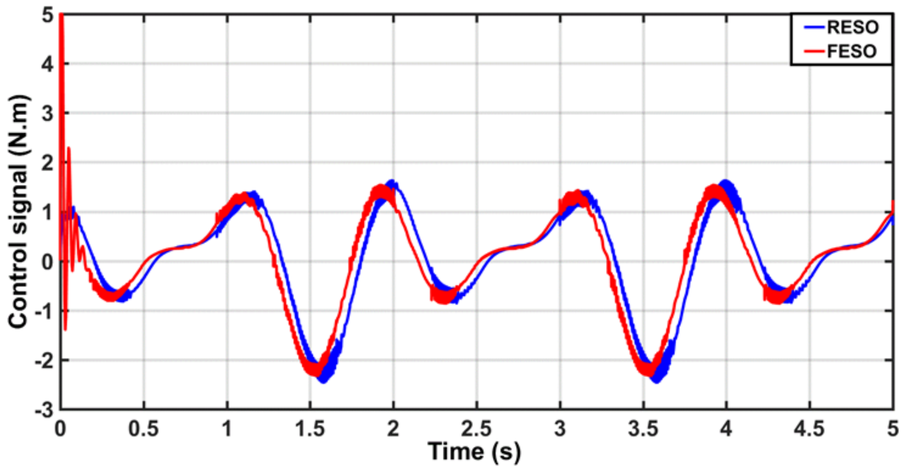

Figure 10. Behaviors of actuating signals based on RESO-based ADRC and FESO-based ADRC with free disturbance.

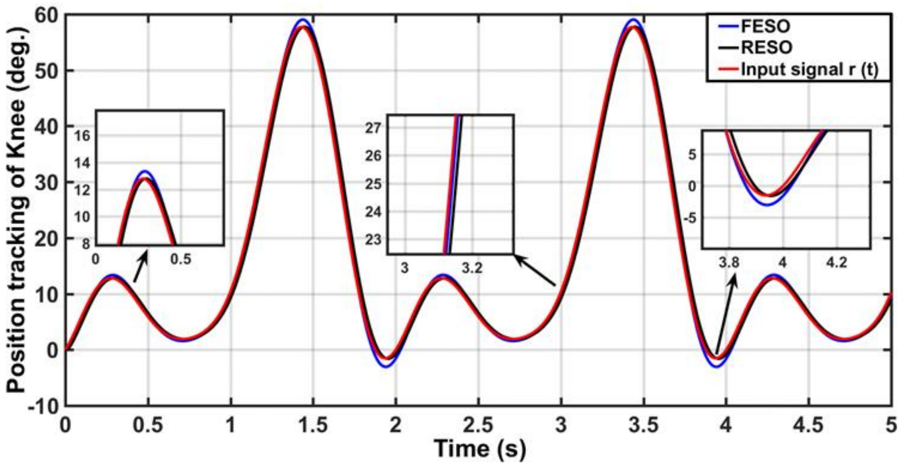

Figure 11. Time responses of knee joint angles based on RESO-based ADRC and FESO-based ADRC subjected to random Gaussian noise load.

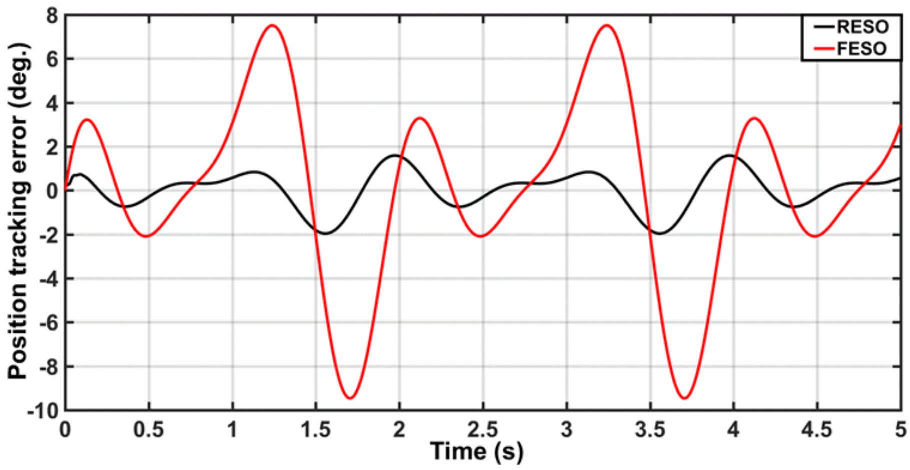

Figure 12. Responses of tracking errors based on RESO-based ADRC and FESO-based ADRC subjected to random Gaussian noise load.

DOI: https://doi.org/10.17509/ijost.v7i2
p- ISSN 2528-1410 e- ISSN 2527-8045

The behaviors of actuating signals have been illustrated in **Figure 13.** There is high spiking at the startup of transient response in the case of FESO-based ADRC, while this chartering disappears in the profile of RESO-based ADRC. This study can be extended for future work either by including recent observation techniques or to design other control schemes either for enhancing the ADRC or for comparison in performance (Hameed, 2017; Humaidi *et al*., 2018b; Sánchez *et al*., 2021; Humaidi & Hameed, 2019a; Laaraba & Khechekhouche, 2018; Humaidi & Abdulkareem 2019b; Pourmahmoud *et al*., 2014; Humaidi *et al*., 2018c; Amli *et al*., 2020; Humaidi etal., 2021; Naima *et al*., 2018; Ajel *et al*., 2021; Mahmoud, 2021; abed *et al*., 2021; Bahatmaka & Kim, 2019; Al-Qadami *et al*., 2020).

7. CONCLUSION

This study presents the design and analysis of ADRC based on RESO for motion control of lower-limb exoskeleton aiding in knee joint flexion-extension exercises. The proposed RESO-based ADRC is compared with ADRC based on FESO. The comparison in performance has been conducted between two control schemes in terms of transient and robustness characteristics via numerical simulation. Both controllers have been tested by applying different reference trajectories and different load profiles. It has been shown that the ADRC based on RESO gives better transient behavior and better load disturbance rejection capabilities. In addition, the control effort produced by RESO-based ADRC shows less chattering in the transient mode of joint angle behavior as compared to other control schemes. The phase lag has substantially reduced due to the proposed controller and the dynamic system of the controlled system is better enhanced.

8. AUTHORS' NOTE

The authors declare that there is no conflict of interest regarding the publication of this article. The authors confirmed that the paper was free of plagiarism.

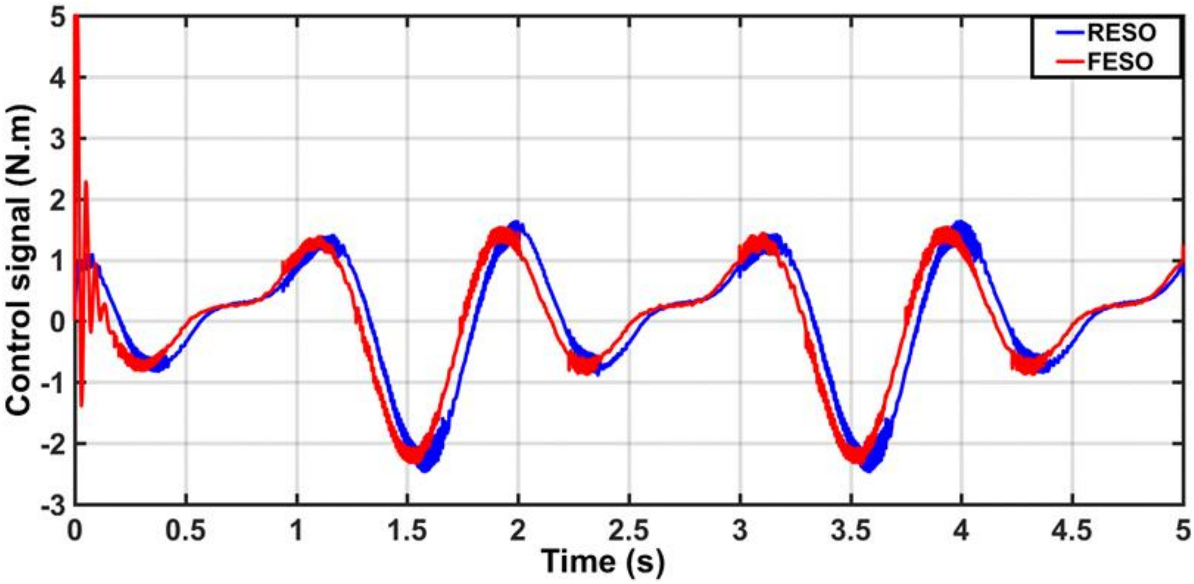

Figure 13. Control signal comparison between RESO and FESO of ADRC subjected to random disturbance

9. REFERENCES

Abed, H.Y., Humod, A.T., and Humaidi, A.J. (2020). Type 1 versus type 2 fuzzy logic speed controllers for brushless DC motors. *International Journal of Electrical and Computer Engineering*, *10*(1), 265–274.

Ajel, A. R., Humaidi, A. J., Ibraheem, I. K., and Azar. A.T. (2021). Robust model reference adaptive control for tail-sitter vtol aircraft. *Actuators*, *10*(7), 162.

Alawad N. A., Amjad J. H., and Al-Araji A. S. (2022). Improved active disturbance rejection control for the knee joint motion model. *Mathematical Modelling of Engineering Problems*, *9*(2), 477-483.

Ali, H. I., Hasan, A. F., and Jassim, H. M. (2020). Optimal H2PID controller design for human swing leg system using cultural algorithm. *Journal of Engineering Science and Technology*, *15*(4), 2270-2288.

Aljuboury, A., and Hameed, A., Ajel, A., Humaidi, A. J., Alkhayyat, A., and Mhdawi, A. (2022). Robust adaptive control of knee exoskeleton-assistant system based on nonlinear disturbance observer. *Actuators*, *11*, 1-18.

Al-Obaidi, A. S. M. (2021a). CDIO initiative: A guarantee for successful accreditation of engineering programmes. *Indonesian Journal of Science and Technology*, *6*(1), 81-92.

Al-Obaidi, A. S. M., Al-Qassar, A., Nasser, A. R., Alkhayyat, A., Humaidi, A. J., and Ibraheem, I. K. (2021b). Embedded design and implementation of mobile robot for surveillance applications. *Indonesian Journal of Science and Technology*, *6*(2), 427-440.

Al-Qadami, E. H., Mustaffa, Z., Abdurrasheed, A. S., Khamaruzaman, W. Y., Shah, S. M. H., and Malek, M. (2020). Numerical assessment on floating stability limits for static vehicle under partial submergence. *Journal of Engineering Science and Technology*, *15*(2), 1384-1398.

Al-Qassar, A. A., Abdulkareem, A. I., Humaidi, A. J., Ibraheem, I. K., Azar, A. T., and Hameed, A. H. (2021a). Grey-wolf optimization better enhances the dynamic performance of roll motion for tail-sitter VTOL aircraft guided and controlled by STSMC. *Journal of Engineering Science and Technology*, *16*(3), 1932-1950.

Al-Qassar, A. A., Al-Dujaili, A. Q., Hasan, A. F., Humaidi, A. J., Ibraheem, I. K., and Azar, A. T. (2021b). Stabilization of single-axis propeller-powered system for aircraft applications based on optimal adaptive control design. *Journal of Engineering Science and Technology*, *16*(3), 1851-1869.

Al-Qassar, A. A., Al-Obaidi, A. S. M., Hasan, A. F., Humaidi, A. J., Nasser, A. R., Alkhayyat, A., and Ibraheem, I. K. (2021c). Finite-time control of wing-rock motion for delta wing aircraft based on whale-optimization algorithm. *Indonesian Journal of Science and Technology*, *6*(3), 441-456.

Amli, A., Sabah, A., Al-Ansari, N., and Laue, J. (2020). Numerical simulation of behaviour of reinforced concrete bars in saturated soil using theoretical models. *Journal of Engineering Science and Technology*, *15*(1), 392-405.

DOI: https://doi.org/10.17509/ijost.v7i2
p- ISSN 2528-1410 e- ISSN 2527-8045

Babalola, E. O., and Omolafe, E. V. (2022a). Construction process of robotic devices to teach aspect of auto mechanic in Nigeria Basic Schools. *ASEAN Journal of Science and Engineering Education, 2*(1)*,* 123-128.

Babalola, E., O., and Omolafe, E., V. (2022b). Detail experimental procedure for the construction process of robotic devices to teach aspect of auto mechanic. *ASEAN Journal of Science and Engineering Education, 2*(2), 169-176.

Bahatmaka, A., and Kim, D. J. (2019). Numerical approach for the traditional fishing vessel analysis of resistance by CFD. *Journal of Engineering Science and Technology*, *14*(1), 207-217.

Bkekri, R., and Benamor, A., Alouane, M., Fried G., and Messaoud, H. (2019). Robust adaptive super twisting controller: methodology and application of a human-driven knee joint orthosis, Industrial Robot. *The International Journal of Robotics Research and Application*, *46*(4), 481-489.

Caifen, F.,and Wen, T. (2021). Analysis and tuning of reduced-order active disturbance rejection control. *Journal of the Franklin Institute*, *358*(1), 339-362.

Castiblanco, P. A., Ramirez, J. L., and Rubiano, A. (2021). Smart materials and their application in robotic hand systems: A state of the art. *Indonesian Journal of Science and Technology*, *6*(2), 401-426.

Djamel, C., and Mefoud, S. (2019). A robust control scheme based on sliding mode observer to drive a knee-Exoskeleton. *Asian Journal of Control*, *21*(1), 439–455.

Eftekhari, H., Al-Obaidi, A. S. M., and Eftekhari, S. (2020). The effect of spoiler shape and setting angle on racing cars aerodynamic performance. *Indonesian Journal of Science and Technology*, *5*(1), 11-20.

Eftekhari, H., Al-Obaidi, A. S. M., and Eftekhari, S. (2023). Aerodynamic performance of vertical and horizontal axis wind turbines: A comparison review. *Indonesian Journal of Science and Technology*, *7*(1), 65-88.

Eftekhari, S., and Al-Obaidi, A. S. M. (2019). Investigation of a cruising fixed wing mini unmanned aerial vehicle performance optimization. *Indonesian Journal of Science and Technology*, *4*(2), 280-293.

Falah, A., Humaidi, A. J., Al-Dujaili, A., and Ibraheem, I. K. (2020). Robust super-twisting sliding control of PAM-actuated manipulator based on perturbation observer. *Cogent Engineering*, *7*(1), 1858393.

Hameed, A.H. (2017). Robustness enhancement of MRAC using modification techniques for speed control of three phase induction motor. *Journal of Electrical Systems*, *13*(4), 723–741.

Hameed, A.H., Al-Dujaili, A.Q., Hussein, H.A. (2019). Design of terminal sliding position control for electronic throttle valve system: A performance comparative study. *International Review of Automatic Control*, *12*(5), 251–260.

Han, J. (1995). A class of extended state observers for uncertain systems. *Control Decision*, *10*(1), 85-88.

DOI: https://doi.org/10.17509/ijost.v7i2
p- ISSN 2528-1410 e- ISSN 2527-8045

Han, J. (1998). Active disturbance rejection controller and its applications. *Control and Decision*, *13*(1), 19-23.

Hassan, F. A., and Rashad, L. J. (2011). Particle swarm optimization for adapting fuzzy logic controller of SPWM inverter fed 3-phase IM. *Engineering and Technology Journal*, *29*(14), 2912-2925.

Hassan, M.Y., Humaidi, A.J., and Hamza, M.K. (2020). On the design of backstepping controller for Acrobot system based on adaptive observer. *International Review of Electrical Engineering*, *15*(4), 328–335.

Huang, Y., and Xue, W. (2014). Active disturbance rejection control: methodology and theoretical analysis. *ISA Transactions*, *53*(4), 963-976.

Humaidi, A.J., and Abdulkareem, A.I. (2019b). Design of augmented nonlinear PD controller of Delta/Par4-like robot. *Journal of Control Science and Engineering*, *2019*, 7689673.

Humaidi, A.J., and Badr, H.M. (2018a). Linear and nonlinear active disturbance rejection controllers for single-link flexible joint robot manipulator based on PSO tuner. *Journal of Engineering Science and Technology Review*, *11*(3), 133–138.

Humaidi, A.J., and Hameed, A.H. (2019a). Design and comparative study of advanced adaptive control schemes for position control of electronic throttle valve. *Information (Switzerland)*, *10*(2), 65.

Humaidi, A.J., Hameed, M.R., and Hameed, A.H. (2018b). Design of block-backstepping controller to ball and arc system based on zero dynamic Theory. *Journal of Engineering Science and Technology*, *13*(7), 2084–2105.

Humaidi, A.J., Hasan, S., and Al-Jodah, A. A. (2018 c). Design of second order sliding mode for glucose regulation systems with disturbance. International Journal of Engineering and Technology (UAE), 7(2), 243–247.

Humaidi, A.J., Kadhim, S. K., and Sharhan A. S. (2022). Optimal adaptive magnetic suspension control of rotary impeller for artificial heart pump. *Cybernetics and Systems*, *53*(1), 141-1167.

Humaidi, A.J., Najem, H. T., Al-Dujaili, A. Q. Pereira, D. A., Ibraheem, K. I. and Azar, A. T. (2021). Social spider optimization algorithm for tuning parameters in PD-like Interval Type-2 Fuzzy Logic Controller applied to a parallel robot. *Measurement and Control*, *54*(3-4) 303–323

Humaidi, A.J.; Kadhim, S. K; and Sharhan A. S. (2020). Development of a novel optimal backstepping control algorithm of magnetic impeller-bearing system for artificial heart ventricle pump. *Cybernetics and Systems*, *51*(4), 521–541.

Khairudin, M., Refalda, R., Yatmono, S., Pramono, H. S., Triatmaja, A. K., and Shah, A. (2020). The mobile robot control in obstacle avoidance using fuzzy logic controller. *Indonesian Journal of Science and Technology*, *5*(3), 334-351.

Kulshreshtha, A., and Al-Obaidi, A. S. M. (2020). Stealth detection system via multistage radar and quantum radar. *Indonesian Journal of Science and Technology*, *5*(3), 470-486.

DOI: https://doi.org/10.17509/ijost.v7i2
p- ISSN 2528-1410 e- ISSN 2527-8045

Laaraba, A., and Khechekhouche, A. (2018). Numerical simulation of natural convection in the air gap of a vertical flat plat thermal solar collector with partitions attached to its glazing. *Indonesian Journal of Science and Technology*, *3*(2), 95-104.

Liu, H., and Li, S. (2012). Speed control for PMSM servo system using predictive functional control and extended state observer. *IEEE on Industrial Electronic*, *59*, 1171-1183.

Long, Y., Du, Z., Cong, L.,Wang,W., Zhang,Z., and Dong, W. (2017). Active disturbance rejection control based human gait tracking for lower extremity rehabilitation exoskeleton. *ISATrans*, *67*, 389-397.

Luay, T. (2020). Optimal tuning of linear quadratic regulator controller using ant colony optimization algorithm for position control of a permanent magnet dc motor. *Iraqi Journal* of *Computers*, *Communication*, *Control* and *System Engineering*, *20*(3), 29-41.

Mahmoud, M. S. (2021). Numerical investigation of conjugate combined convective heat transfer for internal laminar flow of AL2O3/water nanofluid through tube–flat plate solar collector. *Journal of Engineering Science and Technology*, *16*(3), 2378-2393.

Mefoued, S. (2015). A second order sliding mode control and a neural network to drive a knee joint actuated orthosis. *Neurocomputing*, *155*, 71-79.

Mustafa S., Omar F., and Qusay F. (2021). A review on path planning algorithms for mobile robots. *Engineering and Technology Journal*, *39*(5), 804-820.

Naima, K., Liazid, A., Tazerout, M., and Bousbaa, H. (2018). Experimental and numerical investigation of combustion behaviour in diesel engine fuelled with waste polyethylene oil. *Journal of Engineering Science and Technology*, *13*(10), 3204-3219.

Nowak, P., Czeczot, J., and Klopot, T. (2018). Robust tuning of a first order reduced Active disturbance rejection controller. *Control Engineering Practice*, *74*, 44-57.

Pourmahmoud, N., Rahimi, M., Rafiee, S. E., and Hassanzadeh, A. (2014). A numerical simulation of the effect of inlet gas temperature on the energy separation in a vortex tube. *Journal of Engineering Science and Technology*, *9*(1), 81-96.

Sánchez, A. R., Del Rio, J. A. S., and Pujol, T. (2021). Numerical study and theoretical comparison of outlet hole geometry for a gravitational vortex turbine. *Indonesian Journal of Science and Technology*, *6*(3), 491-506.

Shawgi, Y. M., Norsinnira, Z. A., and Zakia, H. (2022). Design and control of a robotic device for upper limb rehabilitation therapy. *Journal of Engineering Science and Technology*, *17*(2), 1306-1327.

Sumit, A., Irraivan, E., and Laxman, W. (2020). Improved active disturbance rejection control for trajectory tracking control of lower limb robotic rehabilitation exoskeleton. *Sensors*, *20*(13), 1-35.

Yang, H., You, X., and Liu, Z. (2015). Extended-state-observer based adaptive control for synchronization of multi-agent systems with unknown nonlinearities. *International Journal of Systems Science*, *46*, 2520–2530.

DOI: https://doi.org/10.17509/ijost.v7i2
p- ISSN 2528-1410 e- ISSN 2527-8045

Yang, H., You, X., Xia, Y., and Li, H. (2014). Adaptive control for attitude synchronisation of spacecraft formation via extended state observer. *IET Control Theory and Applications*, *8*(18), 2171-2185.

Yung, C.P., Tien, D.T.K., and Mahdi Al-Obaidi, A.S. (2016). Delivering holistic education using engineering curriculum through personalized learning, pedagogy, technology and space, *Journal of Engineering Science and Technology*, *11* (Special Issue on the four the ureca 2015), 27–45.

Zhou, X., Tian,C., and Youjie, M. (2013). SHAPF model based on LADRC and its current tracking control. *Electric Power Automation Equipment*, *33*, 49–54.

DOI: https://doi.org/10.17509/ijost.v7i2
p- ISSN 2528-1410 e- ISSN 2527-8045